Stem Cell Reports
Article

ISSCR

OPEN ACCESS

# Bone Morphogenetic Protein 9 Regulates Early Lymphatic-Specified Endothelial Cell Expansion during Mouse Embryonic Stem Cell Differentiation

Mariela Subileau,[1] Galina Merdzhanova,[1] Delphine Ciais,[1,2] Véronique Collin-Faure,[1] Jean-Jacques Feige,[1] Sabine Bailly,[1] and Daniel Vittet[1,*]

[1]Univ. Grenoble Alpes, Inserm, CEA, BIG-BCI, Grenoble 38000, France
[2]Present address: Univ. Côte d'Azur, CNRS, Inserm, iBV, 06189 Nice, France
*Correspondence: daniel.vittet@cea.fr
https://doi.org/10.1016/j.stemcr.2018.11.024

## SUMMARY

Exogenous cues involved in the regulation of the initial steps of lymphatic endothelial development remain largely unknown. We have used an *in vitro* model based on the co-culture of vascular precursors derived from mouse embryonic stem cell (ESC) differentiation and OP9 stromal cells to examine the first steps of lymphatic specification and expansion. We found that bone morphogenetic protein 9 (BMP9) induced a dose-dependent biphasic effect on ESC-derived vascular precursors. At low concentrations, below 1 ng/mL, BMP9 expands the LYVE-1-positive lymphatic progeny and activates the calcineurin phosphatase/NFATc1 signaling pathway. In contrast, higher BMP9 concentrations preferentially enhance the formation of LYVE-1-negative endothelial cells. This effect results from an OP9 stromal cell-mediated VEGF-A secretion. RNA-silencing experiments indicate specific involvement of ALK1 and ALK2 receptors in these different BMP9 responses. BMP9 at low concentrations may be a useful tool to generate lymphatic endothelial cells from stem cells for cell-replacement strategies.

## INTRODUCTION

The lymphatic vascular system is essential for immune surveillance and for the regulation of interstitial tissue fluid homeostasis. Defects in lymphatic development and/or dysfunction of lymphatic vessels are associated with the pathogenesis of several diseases (Aspelund et al., 2016). In particular, lymphatic vascular insufficiency can lead to lymphedema, a disabling disorder characterized by lymphatic fluid stasis and tissue swelling, mostly affecting the extremities (Jiang et al., 2018). Secondary lymphedema is commonly observed after surgery and radiotherapy of breast cancer. Although first-line decongestive and, in more severe cases, surgical therapies have proved useful in reducing edema, no efficient curative treatment currently exists (Shaitelman et al., 2015). Microsurgical lymphatic reconstruction procedures such as lymphatic venous anastomosis and vascularized lymph node transfer are other therapeutic options for the management of lymphedema, but some complications may occasionally develop (Shaitelman et al., 2015). Another promising approach would be to regenerate the damaged lymphatic vasculature by cell-based therapies (Qi and Pan, 2015). Embryonic and tissue stem cells have been postulated to be interesting sources of lymphatic derivatives that could be useful for cell replacement and lymphatic regeneration (Lee et al., 2015; Qi and Pan, 2015; Toyserkani et al., 2015). Several signaling pathways and molecular factors involved in lymphatic vessel development and lymphangiogenesis have been identified. However, the factors involved in the regulation of the initiation of lymphatic vessel development remain poorly characterized.

In the mouse embryo, until very recently the dogma prevailed that the lymphatic system mainly originates from embryonic veins. Several studies have indeed shown that lymphatic specification could be observed since embryonic day 9.5 (E9.5) in a subset of cells in the wall of the cardinal vein. These cells started to express PROX-1, under the control of COUP-TFII and SOX18 (for review, see Semo et al., 2016). Further lymphatic differentiation and lymph sac morphogenesis, occurring under the control of vascular endothelial growth factor C (VEGF-C) stimulation, was observable at E11.5. A role for NFATc1 has also been postulated during these processes, this transcription factor being expressed in endothelial cells undergoing lymphatic fate specification and in lymphatic cells constituting the primary lymph sacs (Kulkarni et al., 2009). Although the veins constitute an important source of lymphatic endothelial cell progenitors, the existence of non-venous sources that can contribute to the development of lymphatic vessels has now also been established for a significant part of the dermal, mesenteric, and heart lymphatic vasculature (for review, see Kazenwadel and Harvey, 2016; Ma and Oliver, 2017). The inductive signals and extracellular factors controlling lymphatic cell-fate specification during embryonic development remain poorly characterized. Only few regulatory pathways have been identified to date (for review, see Semo et al., 2016). Both retinoic acid and ERK signaling have been established as positive regulators of the transcriptional program leading to lymphatic differentiation from the venous vasculature in the mouse embryo (for

 

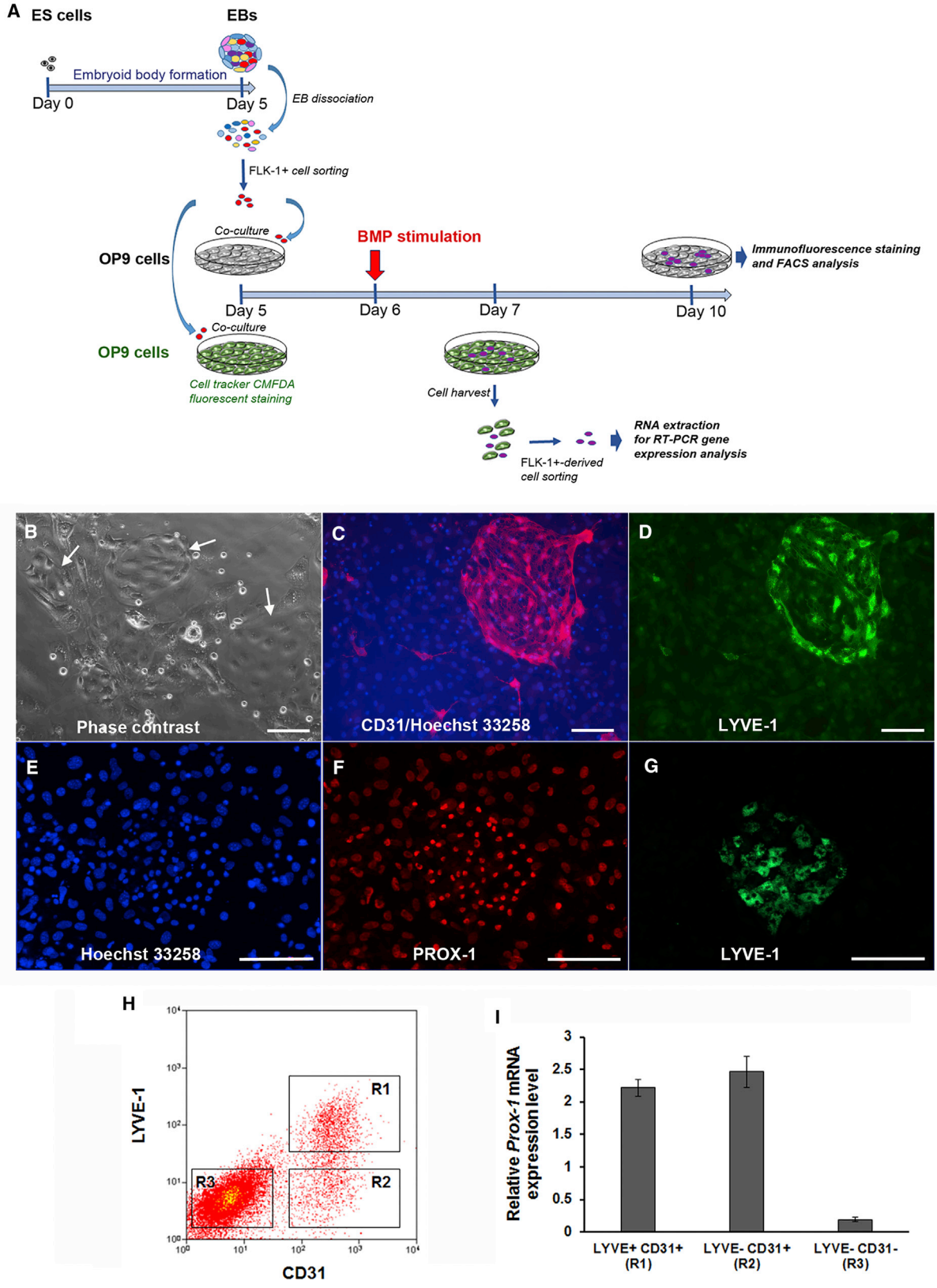


*(legend on next page)*

review, see Semo et al., 2016). Such an effect is also reported for WNT5B, described as an inducer of lymphatic cell fate in both zebrafish and human embryonic stem cells (ESCs) (for review, see Semo et al., 2016). In contrast, NOTCH signaling and the proangiogenic bone morphogenetic protein 2 (BMP2) have been identified as negative regulators of lymphatic specification (Dunworth et al., 2014; Murtomaki et al., 2013).

Mouse ESC differentiation has been previously demonstrated to constitute a useful tool to identify molecular pathways involved in vascular development. Indeed, the early steps of vascular differentiation are recapitulated by this model (for review, see Jakobsson et al., 2007). Moreover, it has also been characterized that the earliest stages of lymphatic development can be observed during mouse ESC differentiation either in embryoid bodies (Kreuger et al., 2006; Liersch et al., 2006) or during co-culture of ESC-derived vascular progenitors on murine OP9 stromal cells (Kono et al., 2006; Vittet et al., 2012).

Bone morphogenetic proteins (BMPs), which have been characterized as essential factors for early embryonic development and stem cell fate (Sieber et al., 2009), appear to be good candidates to exert a role in the early lymphatic differentiation process. Some BMPs have emerged as potent regulators of vascular development and/or angiogenesis (Goumans et al., 2018). Except the inhibitory BMP2 effect reported above (Dunworth et al., 2014), whose action was postulated to be mediated by PROX-1 inhibition, the potential effects of BMPs on lymphatic development have not been addressed to date. While BMP9 was originally described as a potent osteogenic factor (Lamplot et al., 2013), it has also recently been found to influence lymphangiogenesis, lymphatic collecting vessel maturation, and valve morphogenesis (Levet et al., 2013; Yoshimatsu et al., 2013). In addition, BMP9 was also found to be involved in the regulation of lymphatic endothelial cell proliferation and endothelial cell plasticity (Yoshimatsu et al., 2013).

In this study, we have investigated the potential role of BMP9 in early lymphatic development using the mouse ESC *in vitro* differentiation model in order to better characterize the initial events governing the expansion of the lymphatic endothelial lineage.

## RESULTS

### Early Steps of Lymphatic Differentiation Take Place during Co-cultures of ESC-Derived FLK-1$^+$ Vascular Precursors on OP9 Stromal Cells

We first performed a series of experiments to confirm and further provide evidence that the *in vitro* experimental differentiation model we used mimics the initial differentiation commitment into the lymphatic endothelial cell lineage. The main steps of the procedure and treatments are illustrated on Figure 1A. As shown on Figure 1B, cell clusters exhibiting an endothelial morphology are obtained from co-cultures of FLK-1$^+$ vascular precursors and OP9 stromal cells. Immunofluorescence staining experiments of these co-cultures revealed that endothelial-like cell clusters are mostly constituted by CD31$^+$ and LYVE-1$^+$ expressing cells. In parallel, the presence of scattered and/or cord-like organized CD31$^+$ LYVE-1$^-$ cells was observed (Figures 1C and 1D). During the first days in co-culture, LYVE-1 expression, previously reported as an indicator of lymphatic endothelial competence, appeared to initiate in a subset of cells that were first expressing CD31 and which seemed to further expand (Figure S1). At day 10 of differentiation, we and others have previously shown that CD31$^+$ LYVE-1$^+$ cells represented a cell population that is committed early toward the lymphatic endothelial lineage (Kono et al., 2006; Vittet et al., 2012). The lymphatic lineage commitment of LYVE-1-positive cells is further supported by the expression of PROX-1, a marker of the endothelial lymphatic identity. PROX-1

**Figure 1. ESC-Derived Vascular Precursors Co-cultured on Murine Stromal OP9 Cells Are Able to Form Early Lymphatic Derivatives**

(A) Schematic of the differentiation protocol illustrating the main steps and specific treatments according to the experiment goals. EBs, embryoid bodies.

(B) Morphological observations of endothelial cell clusters formed after 5 days of co-culture (day 10 of differentiation) in control conditions. The arrows point to cell clusters exhibiting an endothelial-like morphology.

(C–G) Immunofluorescence staining of endothelial cell-like clusters obtained in unstimulated control conditions at day 10/11 with anti-CD31 (C), anti-LYVE-1 (D and G), and anti-PROX-1 (F) antibodies. Nuclei were counterstained with Hoechst 33258 (C and E). Scale bars, 100 μm.

(H) Flow-cytometry dot plot of the LYVE-1 and CD31 double immunostaining of the co-cultures at day10/11 used for cell sorting. The different gates used are outlined: R1, CD31$^+$/LYVE-1$^+$ cells; R2, CD31$^+$/LYVE-1$^-$ cells; R3, CD31$^-$/LYVE-1$^-$ cells. Co-cultures were performed in the presence of 0.3 ng/mL BMP9 to obtain sufficient cell numbers in the LYVE-1$^+$ and LYVE-1$^-$ cell fraction.

(I) Relative *Prox-1* mRNA expression levels. Data shown are the mean ± SD of triplicates from the qRT-PCR experiment performed with the RNAs extracted from the different cell populations gated on the dot plot of the experiment illustrated in (H).

See also Figure S1.

expression in LYVE-1-positive cells was detected both by immunofluorescence staining (Figures 1E–1G) and by qRT-PCR experiments (Figures 1H and 1I). Unexpectedly, CD31$^+$ LYVE-1$^-$ cells were also displaying a *Prox-1* expression (Figures 1H and 1I), which might correspond to a putative early differentiation step preceding the LYVE-1 expression differentiation stage.

### BMP9 Expands ESC-Derived CD31$^+$ LYVE-1$^+$ Early Lymphatic-Specified Endothelial Cell Population

We then asked whether BMP9 could affect lymphatic endothelial differentiation from FLK-1-positive ESC-derived vascular precursors. ESC-derived FLK-1-positive vascular precursors were co-cultured on OP9 stromal cells for 24 hr before treatment in the presence of different concentrations of the tested agents for another period of 4 days. Quantitative flow-cytometry analysis showed that BMP9 exerted a bell-shaped dose-dependent effect on the formation of LYVE-1-positive cells, eliciting a 2-fold increase over control. A peak in the percentage of LYVE-1-positive cells was observed at 0.3 ng/mL, while at 10 ng/mL the BMP9 response was similar to that of the untreated control (Figure 2A). Consistent with this analysis, we noticed that the formation of LYVE-1-positive endothelial sheet-like cell clusters were larger after treatment with 0.3 ng/mL BMP9 (Figure S2). Interestingly, BMP10, which is the member closest to BMP9 (Garcia de Vinuesa et al., 2016), gave a similar profile response (Figure 2A). In contrast, at similar concentrations BMP2 did not increase the formation of LYVE-1-positive cells, whereas at 50 ng/mL it significantly inhibited this process (Figure 2A).

Another series of experiments, depicted in Figure 2B, was performed to characterize the kinetics of the BMP9 effect and to determine whether the BMP9-induced increase in LYVE-1-positive cell population resulted from the activation of a proliferation process. After a single BMP9 addition at day 6, a significant increase in the LYVE-1$^+$ cell population was only observed beyond day 8 (Figure 2C). Bromodeoxyuridine (BrdU) incorporation studies with pulse labeling of the cells in co-culture at day 7 or day 8 revealed that BMP9 significantly activated the proliferation of the LYVE-1-positive cell population at day 8, eliciting more than a 1.5-fold rise over control (Figure 2D). Such an increase in BrdU incorporation in response to BMP9 was not observed at day 7.

### BMP9 Activates FLK-1$^+$ Vascular Precursors and Interferes with the Calcineurin/NFATc1 Signaling Pathway

The canonical BMP signaling pathway downstream of type I receptors leads to the phosphorylation of SMAD1/5 proteins. We then investigated the effect of the addition of 0.1 ng/mL BMP9, a dose in the range of those inducing LYVE-1-positive cell formation, on SMAD1/5 phosphorylation in FLK-1-positive sorted vascular precursors. A high SMAD1/5 phosphorylation level was obtained in response to 0.1 ng/mL BMP9 in FLK-1-positive sorted vascular precursors at day 5, but not in OP9 cells (Figure S3). These observations are consistent with a functional coupling of BMP9 with phosphorylation of SMAD1/5 proteins on FLK-1-positive cells, which could activate the initial stages of the differentiation process, leading to the further expansion of the endothelial lymphatic lineage.

We next investigated whether BMP9 regulates the expression of transcription factors (COUP-TFII, SOX18, and PROX-1) known to be involved in the commitment and the early differentiation into the lymphatic endothelial cell lineage (for review, see Ma and Oliver, 2017; Semo et al., 2016). We measured by qRT-PCR their expression levels after a 24-hr stimulation by 0.3 ng/mL BMP9. As a positive control of the efficiency of the BMP9 treatment, we looked at the expression level of *Smad6* that has been shown to be induced by BMP9 in primary lymphatic endothelial cell culture (Niessen et al., 2010). The expressions of *Coup-tfII*, *Sox18*, and *Prox-1* in vascular progenitors were unchanged after BMP9 stimulation (Figure 3A). Moreover, no significant variation in *Prox-1* expression was observed after 4 hr of BMP9 stimulation on FLK-1$^+$ vascular precursors (data not shown). This time point was investigated since a BMP9-induced transient regulation of *Prox-1* expression, which lasted only a few hours, was reported in previous studies performed on adult lymphatic endothelial cells (Levet et al., 2013; Yoshimatsu et al., 2013).

We also investigated whether the transcription factor NFATc1, which has been established to be involved in lymphatic vascular development (Kulkarni et al., 2009), could be a target for BMP9. We found that *Nfatc1* gene expression was slightly but significantly induced, in response to 24-hr stimulation with 0.3 ng/mL BMP9, in ESC-derived vascular derivatives in co-culture with OP9 stromal cells (Figure 3A). That calcineurin phosphatase/NFATc1 signaling pathway as a target for BMP9 was further confirmed at the protein level on FLK-1$^+$ vascular precursors. As illustrated in Figure 3B, a higher NFATc1 protein level was measured after 20 min of stimulation with 0.3 ng/mL BMP9.

Moreover, to demonstrate that calcineurin-NFATc1 signaling may be involved in the control of LYVE-1-positive cell formation induced by low doses of BMP9, we performed the experiments in the presence of cyclosporin A, an inhibitor of calcineurin phosphatase activity and thereby of NFATc1 signaling (Horsley and Pavlath, 2002). We observed that cyclosporin A significantly inhibits

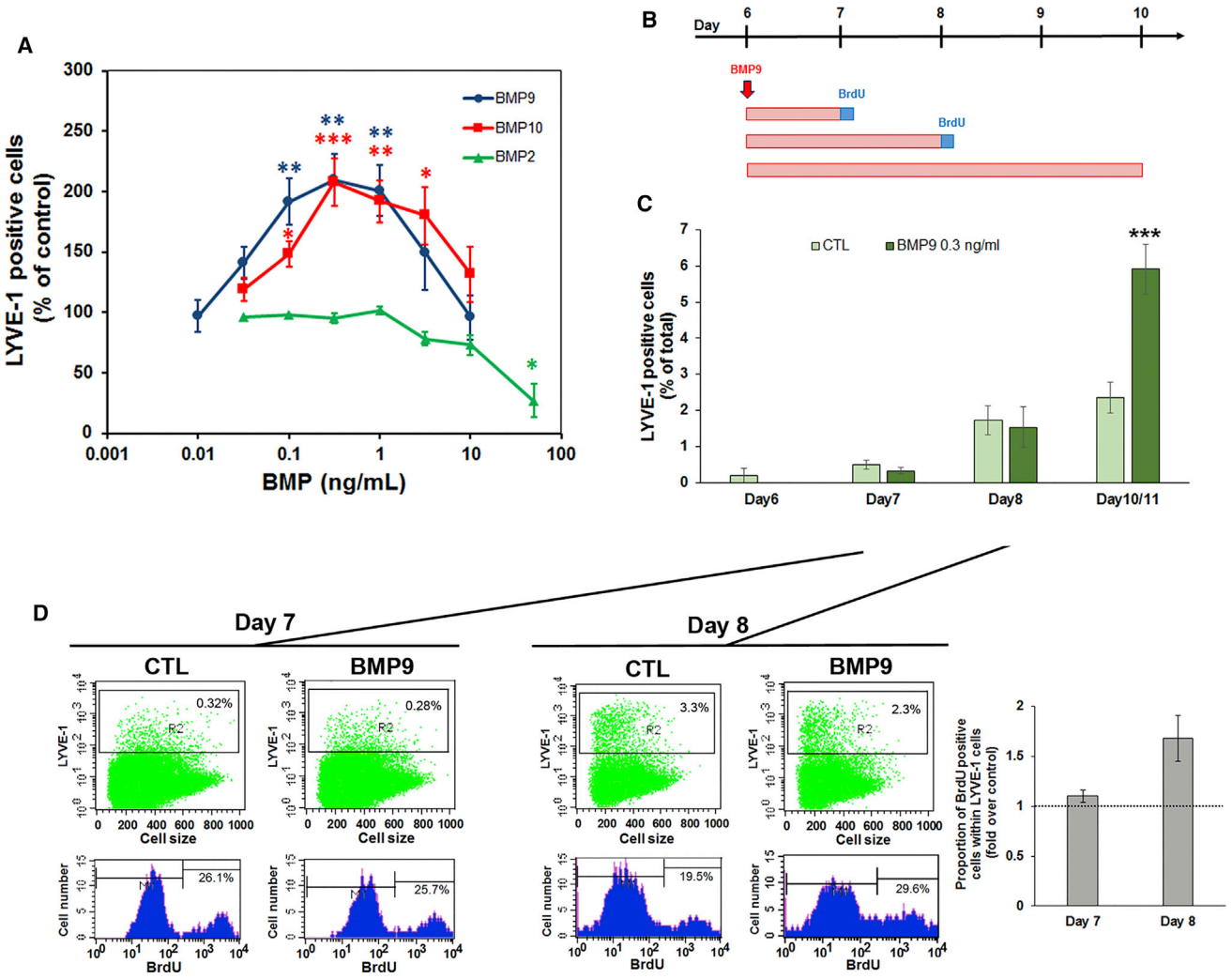


**Figure 2. BMP9 Increases the Formation of LYVE-1$^+$ Cells during the Co-culture of ESC-Derived Vascular Precursors on Murine Stromal OP9 Cells**

(A) Flow-cytometry analysis of the formation of LYVE-1$^+$ early lymphatic-specified endothelial cells from co-cultures of FLK-1$^+$ vascular precursors on OP9 stromal cells, in response to variable concentrations of BMPs. Vascular precursors were plated on OP9 stromal cells at day 5, and BMPs were added under serum-free conditions after 24 hr of co-culture. The formation of LYVE-1-positive cells was measured at day 10 (after 4 days of stimulation with BMPs). Data are the mean ± SEM of 4 (BMP2), 8 (BMP10), or 11 (BMP9) different experiments. ***$p < 0.001$, **$p < 0.01$, *$p < 0.05$, significantly different from basal control values using an unpaired Student's t test.

(B) Schematic of the differentiation kinetics protocol with the different time points used for pulse labeling with BrdU.

(C) Flow-cytometry analysis of the formation of LYVE-1-positive cells in the absence (CTL) or in the presence of 0.3 ng/mL BMP9 added at day 6. The reported data originated from pooled different experiments. They are the mean values ± SEM obtained from 2 (Day6), 5 (Day7 and Day8), and 8 (Day10/11) different sets of values, according to the considered time point. ***$p < 0.001$, significantly different from its respective control using unpaired Student's t test.

(D) Representative flow-cytometry charts of pulse BrdU labeling of the co-cultures after 24 hr (Day 7) and 48 hr (Day 8) without (CTL) or after BMP9 (0.3 ng/mL) stimulation. The upper dot plots illustrate the LYVE-1 cell immunoreactivity (LYVE-1-positive cells are gated in R2), and the lower histogram plots show BrdU immunoreactivity of the R2-gated LYVE-1-positive cell population. The percentage of positive cells is indicated on each plot. The BMP9 fold stimulation of BrdU incorporation in LYVE-1-positive cells is reported in the right histogram chart and presented as the mean ± SD of two independent experiments.

See also Figure S2.

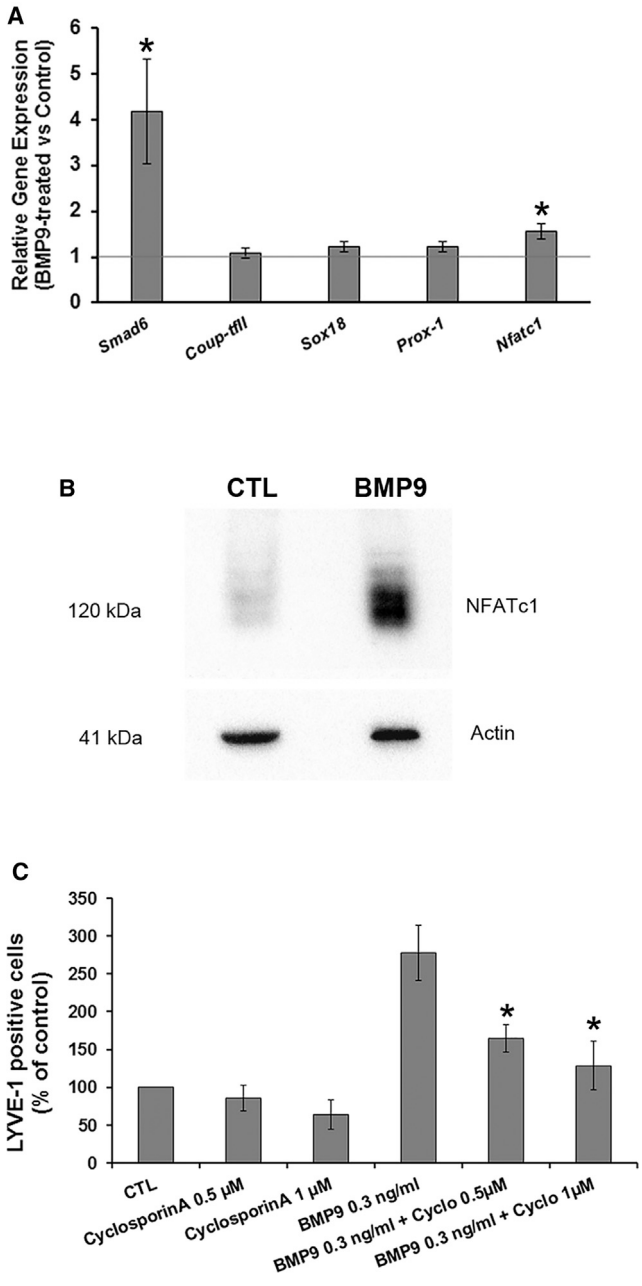


**Figure 3. Low Concentrations of BMP9 Modulate the Calcineurin/NFATc1 Signaling Pathway**

(A) qRT-PCR analysis of BMP9 effects on the mRNA levels of transcription factors known to be essential for lymphatic differentiation. FLK-1$^+$ vascular precursors at day 5 were plated on CellTracker CMFDA-stained OP9 stromal cells. BMP9 (0.3 ng/mL) was added at day 6. After 24 hr of treatment, the CMFDA-negative cell population was sorted and collected for gene expression analysis. Data are the mean ± SEM of five experiments.

(B) NFATc1 protein expression analysis after BMP9 stimulation. FLK-1$^+$ vascular precursors at day 5 were stimulated in suspension in serum-free medium with or without 0.3 ng/mL BMP9 for 20 min. Immunoblotting was performed using an antibody against NFATc1 or actin proteins as a loading control. Results of a representative experiment, out of three, are illustrated. Sizes of the molecular weight markers are indicated on the left.

(C) Inhibition of NFATc1 signaling by cyclosporin A prevents the BMP9-induced increase in LYVE-1$^+$ cell formation. LYVE-1-positive cell formation was measured by flow cytometry 4 days after addition of BMP9 in the absence or presence of cyclosporin A. Data are the mean ± SEM of three experiments.

*$p < 0.05$, significantly different from control untreated cells (A) and significantly different from treatment with BMP9 alone (C) using unpaired Student's t test. See also Figure S3.

BMP9-induced LYVE-1-positive endothelial cell expansion, further supporting a role of NFATc1 in the response elicited by BMP9 (Figure 3C).

## High Concentrations of BMP9 Direct ESC-Derived Vascular Progenitor Differentiation toward LYVE-1-Negative Endothelial Cells through Potential Involvement of VEGF-A

Since a previous work reported that 1 ng/mL BMP9 can regulate endothelial cell fate of mature endothelial cells (Yoshimatsu et al., 2013), we then wondered whether the decrease in LYVE-1-positive cell formation toward basal control level, observed after the treatment with high BMP9 concentrations (Figure 2A), could reflect a preferential commitment toward another endothelial lineage or another endothelial cell differentiation stage. We found that BMP9, at concentrations above 0.5 ng/mL, significantly increased in a dose-dependent manner the formation of CD31$^+$ LYVE-1$^-$ cells (Figures 4A and 4B). This effect was not observed for BMP10 or BMP2 (Figure 4A).

A recent study described the induction of VEGF-A synthesis and secretion in mesenchymal stem cells in response to BMP9 (Ai et al., 2015). A constitutive *Vegf-A* expression by OP9 stromal cells has also been reported and was found to be enhanced when ESC-derived endothelial cells were co-cultured with OP9 cells (Matsumura et al., 2003). We therefore wondered whether the induction of CD31$^+$ LYVE-1$^-$ endothelial cell formation observed at high BMP9 concentrations could be mediated by VEGF-A. First, we tested the effects of VEGF-A addition in the co-cultures of FLK-1-positive vascular precursors and OP9 stromal cells. As reported in Figure 5A, we observed a dose-dependent induction of the formation of CD31$^+$ LYVE-1$^-$ cells in response to VEGF-A. Interestingly, this differentiation occurred at the expense of the LYVE-1-positive cell population since an inhibition of the formation of LYVE-1-positive cells was found in parallel (Figure 5A). Although a VEGF-A-induced proliferative effect may probably also contribute to the CD31$^+$ LYVE-1$^-$ cell rise, a major VEGF-A effect was seen on the

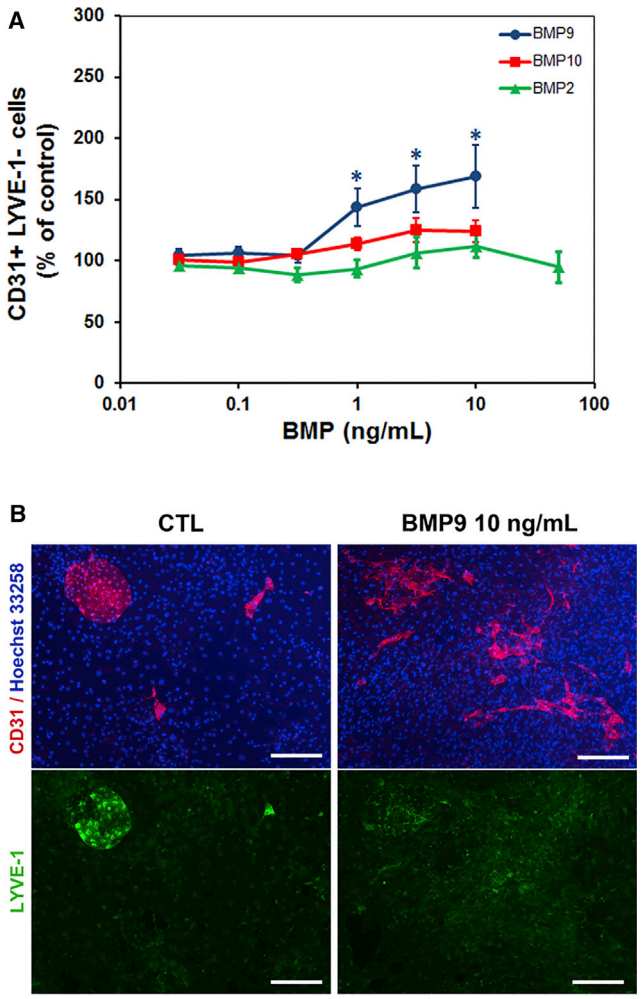


**Figure 4. Analysis of CD31$^+$ LYVE-1$^-$ Endothelial Cell Formation during the Co-culture of ESC-Derived Vascular Precursors on Murine Stromal OP9 Cells**

(A) Flow cytometry quantitative measurement of CD31$^+$ LYVE-1$^-$ cell formation after co-culture of FLK-1$^+$ vascular precursors on OP9 stromal cells in response to variable concentrations of BMP9. Data are the mean ± SEM of 4 (BMP2), 8 (BMP10), or 11 (BMP9) different experiments. *$p < 0.05$, significantly different from basal control values using an unpaired Student's t test.

(B) Immunofluorescence staining with anti-CD31 and anti-LYVE-1 antibodies of cell co-cultures at day 10 of differentiation, in the absence (CTL) or presence of 10 ng/mL BMP9. Scale bars, 200 μm.

endothelial cell repartition between the two cell populations, without significant variations in the total number of endothelial cells (Figure 5B).

We next investigated whether the effects of BMP9 (10 ng/mL) could be mediated through VEGF-A, and analyzed by ELISA the presence of VEGF-A in the supernatant of ESC-derived FLK-1$^+$ cells co-cultured on OP9. We found that VEGF-A was secreted at low levels during the co-culture of ESC-derived precursors on OP9 stromal cells (Figure 5C) and that BMP9 treatment at 10 ng/mL significantly induced VEGF-A secretion, increasing by nearly 2-fold. The involvement of VEGF-A in the BMP9 response was supported by the use of VEGF-A neutralizing antibodies in the co-culture differentiation protocol, which inhibited the BMP9-induced formation of CD31$^+$ LYVE-1$^-$ cells (Figure 5D). As a control, this antibody was observed to partially block the CD31$^+$ LYVE-1$^-$ cell differentiation response induced by the addition of human recombinant VEGF-A (data not shown). To identify the cellular origin of VEGF-A induced by BMP9 in the culture medium, we conceived the hypothesis that OP9 stromal cells could constitute a potential source. We first investigated a potential BMP9 functional coupling with phosphorylation of SMAD1/5 proteins in OP9 cells at high BMP9 concentrations. OP9 cells were serum-starved for 1 hr before stimulation with or without BMP9. We found a marked SMAD1/5 phosphorylation in response to treatment with 10 ng/mL BMP9 for 1 hr (Figure 5E). We also observed that BMP9 induces a 2-fold increase in VEGF-A secretion by OP9 stromal cells after 48 hr of stimulation (Figure 5F).

## Differential Involvement of BMP9 Type I Receptors in CD31$^+$ LYVE-1$^-$ and CD31$^+$ LYVE-1$^+$ Cell Populations Formation from ESC-Derived Vascular Precursors in Co-culture with OP9 Stromal Cells

We then wondered whether the different specific responses elicited by low and high BMP9 concentrations may be the result of differential receptor mobilization. Two type I receptors are currently described to be activated by BMP9: ALK1 and ALK2 (for review, see Garcia de Vinuesa et al., 2016; Goumans et al., 2018). We found a major *Alk1* mRNA expression level against *Alk2* in FLK-1$^+$ cells (Figure S4A). On the other hand, a predominant *Alk2* mRNA expression was observed in OP9 cells compared with *Alk1*, which remained barely expressed (Figure S4A). We then performed RNA-silencing experiments and first checked knockdown efficiencies at the time points post transfection when cells were stimulated by BMP9 (Figures S4B and S4C).

Lymphatic endothelial cell development in response to 0.3 ng/mL BMP9 was then examined, after small interfering RNA (siRNA) transfection either in FLK-1$^+$ precursor cells or in both precursors and OP9 cells. We found that the BMP9-induced LYVE-1-positive cell formation was partially but significantly inhibited after *Alk1* silencing but was not affected by *Alk2* knockdown (Figure 6A). On the other hand we found that, when RNA silencing was conducted in OP9 cells, the knockdown of *Alk2* prevented the increase in the formation of CD31$^+$ LYVE-1$^-$ endothelial cells induced by high BMP9 concentrations in the co-cultures of FLK-1$^+$ vascular precursors on these OP9 transfected cells

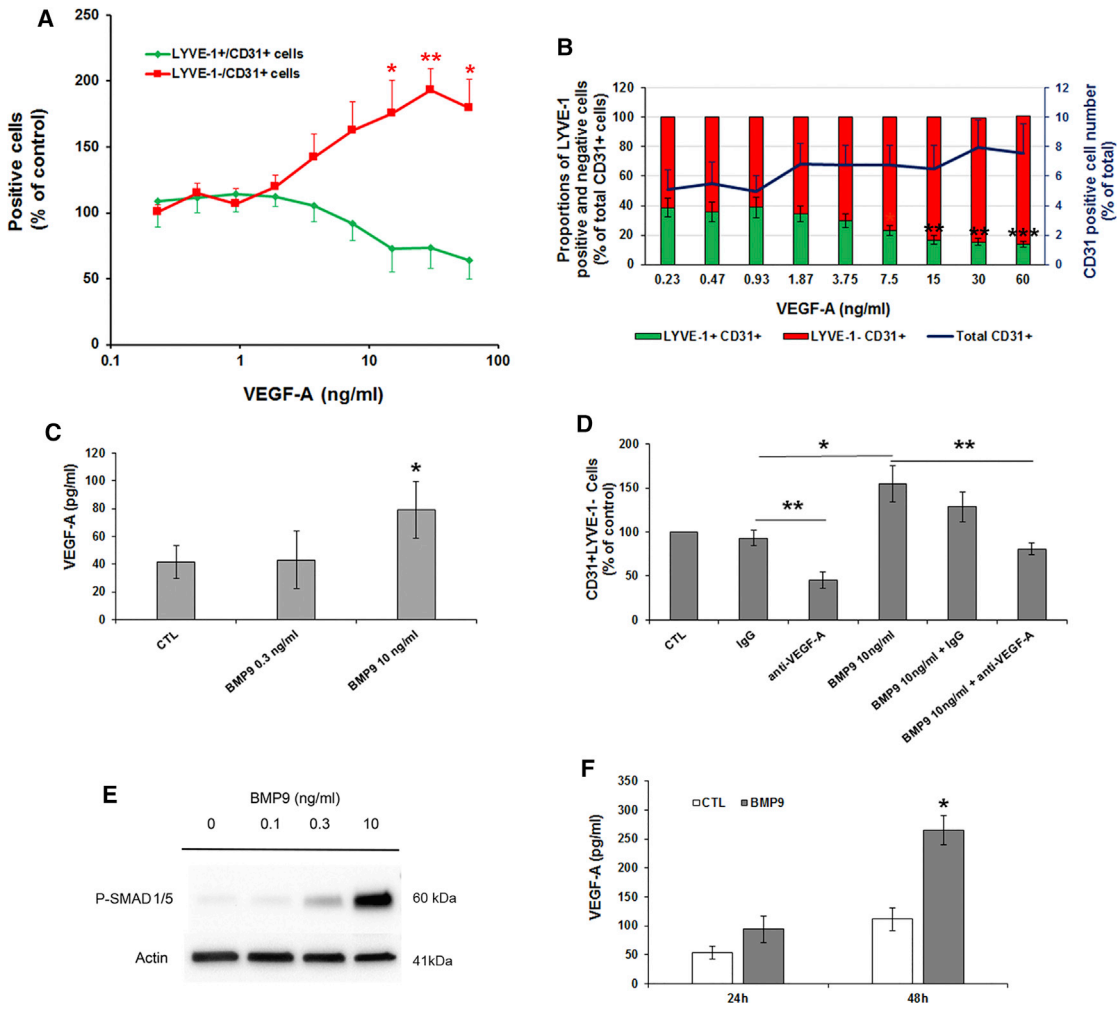


**Figure 5. VEGF-A Regulates Endothelial Differentiation from ESC-Derived Vascular Precursors and Mediates the Effects of High BMP9 Concentrations**

(A) Quantitative flow-cytometry analysis of the formation of CD31$^+$ LYVE-1$^-$ and CD31$^+$ LYVE-1$^+$ cells in response to variable doses of VEGF-A. Data are the mean ± SEM of five different experiments.

(B) Dose-dependent VEGF-A effects on the formation of CD31-positive endothelial cells (blue line) and on their repartition between LYVE-1$^+$ early lymphatic specified (green bars) and LYVE-1$^-$ (red bars) endothelial cells. Data are the mean ± SEM from five or six experiments.

(C) VEGF-A production in the co-culture differentiation medium. VEGF-A levels were measured by ELISA after 48 hr of treatment with the indicated agents. Values are the mean ± SD values from 2–3 experiments.

(D) Anti-VEGF-A neutralizing antibody inhibits control and BMP9-induced CD31$^+$ LYVE-1$^-$ cell formation from ESC-derived vascular precursors in co-culture on OP9 stromal cells. Data are the mean ± SEM of five experiments.

(E) BMP9 functional coupling with SMAD1/5 phosphorylation in OP9 stromal cells. Serum-starved subconfluent OP9 cells were stimulated for 1 hr in the absence (CTL) or presence of variable BMP9 concentrations. Immunoblots with phospho SMAD1/5 antibodies and actin antibodies for normalization are illustrated.

(F) Effects of 10 ng/mL BMP9 on VEGF-A production by OP9 cells. Data are the mean ± SEM of seven experiments.

*p < 0.05, **p < 0.01, ***p < 0.001, significantly different from respective controls or as indicated, using unpaired Student's t test.

(Figure 6B). We also observed in parallel, that *Alk2* silencing in OP9 cells blocked SMAD1/5 phosphorylation and VEGF-A secretion induced by 10 ng/mL BMP9, whereas *Alk1* silencing did not interfere with these responses (Figures 6C and 6D).

## DISCUSSION

In this study, we found that BMP9 increases the expansion of LYVE-1-positive early lymphatic-specified endothelial cells during mouse ESC differentiation in a bell-shaped

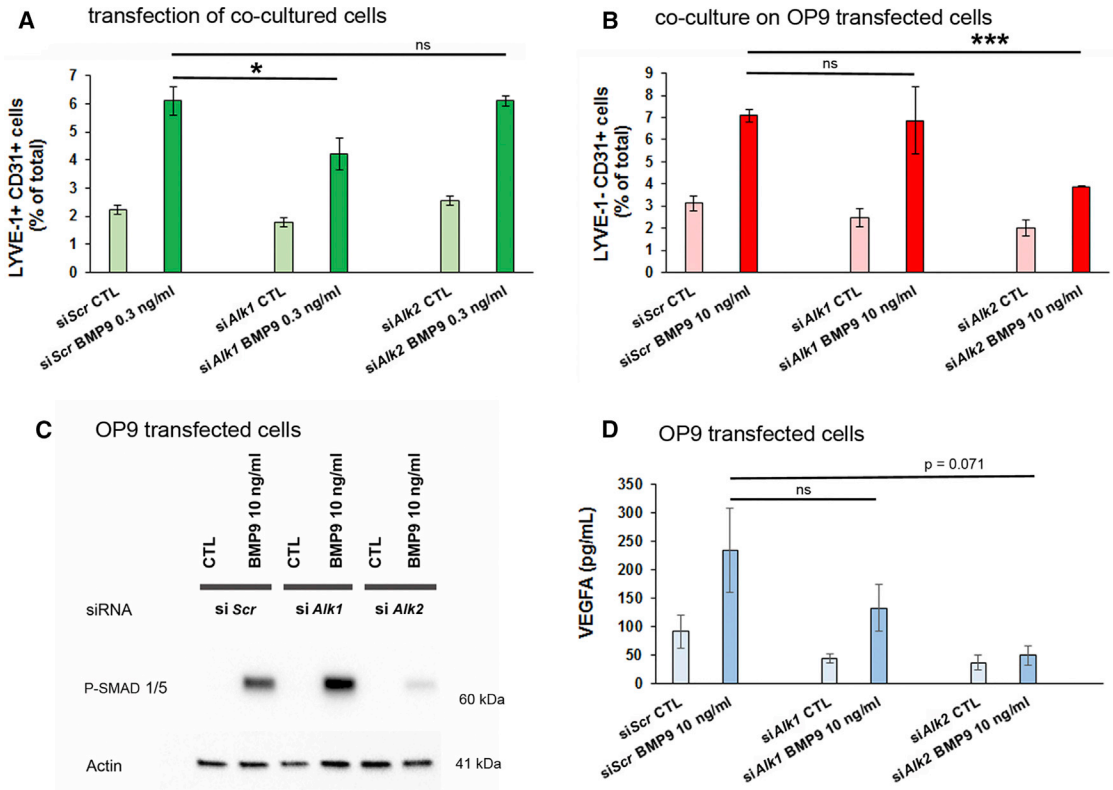


**Figure 6. Analysis of Differential BMP Type I Receptor Involvement in the BMP9 Low-Dose and High-Dose Effects by RNA-Silencing Experiments**

(A) Effect of *Alk1* and *Alk2* siRNA on LYVE-1-positive cell formation induced by 0.3 ng/mL BMP9 in FLK-1$^+$ vascular precursor co-cultures on mouse OP9 cells. *Alk* knockdowns were performed by siRNA transfection of vascular precursors by either electroporation or by using Lipofectamine RNAiMAX, 24 hr before BMP9 stimulation. Data are the mean ± SEM of three (si*Alk2*) or four (si*Scr*, si*Alk1*) different experiments.

(B) High-dose BMP9-induced LYVE-1$^-$ endothelial cell formation is inhibited after prior *Alk2* knockdown in OP9 cells. OP9 cells were first transfected by Lipofectamine RNAiMAX with the different siRNAs, 24 hr before FLK-1$^+$ vascular precursor plating in co-culture on OP9 cells and 48 hr before stimulation with 10 ng/mL BMP9. LYVE-1$^-$ CD31$^+$ cell formation is illustrated. Data are the mean ± SEM of three experiments.

(C and D) *Alk2* knockdown in OP9 cells prevents SMAD1/5 phosphorylation and VEGF-A secretion induced by 10 ng/mL BMP9. OP9 cells were transfected with the different siRNAs by Lipofectamine RNAiMAX, 48 hr before stimulation with 10 ng/mL BMP9. For SMAD1/5 phosphorylation studies, serum-starved subconfluent OP9 cells were stimulated for 1 hr in the absence (CTL) or presence of BMP9, before immunoblotting with anti P-SMAD1/5 and actin antibodies (C). VEGF-A levels were measured after 48 hr of treatment with or without 10 ng/mL BMP9, by ELISA (D). Data are mean ± SEM of three experiments.

*$p < 0.05$, ***$p < 0.001$, significantly different from BMP9 stimulation obtained after transfection with siScramble (si*Scr*), using unpaired Student's t test. See also Figure S4.

dose-dependent manner. At low doses, BMP9 increases the formation of LYVE-1-positive endothelial cell derivatives, at least in part via the calcineurin phosphatase/NFATc1 signaling pathway. In contrast, high BMP9 doses, by promoting in addition the VEGF-A secretion by OP9 cells, result in the induction of LYVE-1-negative endothelial cell formation. RNA-silencing experiments indicate specific involvement of distinct type I BMP receptor subtypes in these different BMP9 effects. We also provide further evidence for *Vegf-A* gene expression being a target of high BMP9 concentrations in stromal cells. A hypothetical model recapitulating our data is illustrated in Figure 7.

Previous *in vitro* studies have reported BMP9 effects on differentiated ESC-derived blood endothelial cells and/or mature blood endothelial cells (David et al., 2007; Rostama et al., 2015; Scharpfenecker et al., 2007; Suzuki et al., 2010). Both positive and negative effects on cell proliferation and/or migration were described, strongly suggesting a cell-context- and dose-dependent effect for BMP9 regulation. In *in vivo* angiogenesis models, BMP9 mostly appears

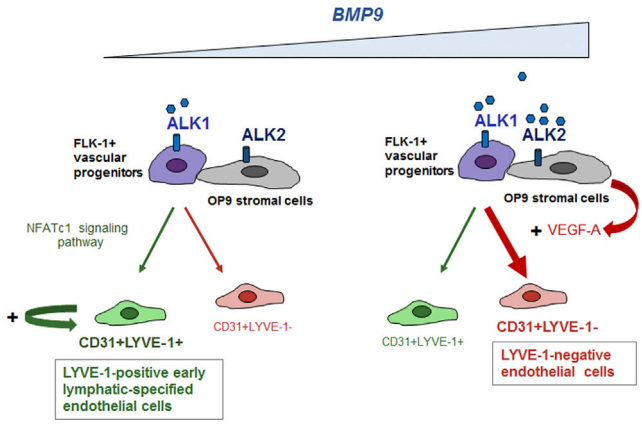


**Figure 7. Hypothetical Model for BMP9 Regulation of ESC-Derived Vascular Precursor Differentiation in Co-culture with Murine OP9 Stromal Cells**

Low BMP9 concentrations induce the formation of LYVE-1$^+$ early lymphatic-specified endothelial cells through ALK1 activation. BMP9 was observed to directly activate FLK-1$^+$ vascular precursors and earlier stages of vascular committed cells through mobilization of the NFATc1 signaling pathway. Moreover, an increase in the proliferation of the LYVE-1-positive cell population was found to largely contribute to its expansion. At higher doses, BMP9 could, in addition to ALK1, also activate ALK2 present on OP9 stromal cells. This leads to a significant rise in the secretion of VEGF-A by OP9 cells, with as a resultant effect an increase in LYVE-1$^-$ endothelial cell population at the expense of the LYVE-1$^+$ early lymphatic-specified endothelial cell formation.

as a vascular endothelial quiescence factor (for review, see Cunha et al., 2017). In this study, we show that BMP9 is also involved in the regulation of the early processes governing LYVE-1-positive lymphatic-specified endothelial cell formation.

Since we previously established a negative effect of transforming growth factor β1 (TGFβ1) on lymph vasculogenesis (Vittet et al., 2012), our results indicate that BMP9 may counterbalance this TGFβ1 inhibitory action. We also identified a pro-lymph-vasculogenic effect for BMP10, the other high-affinity ligand for ALK1, to a similar extent to BMP9. On the other hand, and as previously reported (Dunworth et al., 2014), we found a slight but significant inhibition in the formation of LYVE-1-positive cells in response to high BMP2 doses. It thus appears that several members of the TGFβ superfamily play critical roles in early lymphatic endothelial expansion and/or cell specification during mouse ESC *in vitro* differentiation.

Concerning the mechanisms and the signaling pathways involved, BrdU incorporation experiments indicate that the stimulation of the proliferation of the early lymphatic-specified LYVE-1-positive cell population contributes to its significant expansion by day 10. Nevertheless, an earlier BMP9 effect could also be involved since we observed that FLK-1$^+$ vascular precursors were direct BMP9 targets, as revealed by the SMAD1/5 protein phosphorylation response experiments. Our results are in accordance with BMP9 effects being in large part mediated by the calcineurin-NFATc1 pathway. A critical role of this pathway is evidenced first by an early increase in *Nfatc1* gene expression in response to the stimulation by 0.3 ng/mL BMP9, and second, by the fact that cyclosporin A, known to block this pathway (Norrmen et al., 2009), reversed the BMP9-induced LYVE-1-positive cell formation during the differentiation of FLK-1$^+$ vascular precursors in co-culture with OP9 stromal cells. Further evidence for an involvement of this pathway is provided at the protein level by the observation of a sustained NFATc1 expression level, which may reflect an increased stability or an increased translation ratio of the protein after BMP9 stimulation. The exact mechanism affecting NFATc1 protein remains to be further elucidated in detail. The involvement of the calcineurin/NFATc1 signaling pathway in lymphatic development has previously been established (Kulkarni et al., 2009). It was shown that NFATc1 can be observed on some endothelial cells of the cardinal vein that are also positive for PROX-1, at the initial stage of lymphatic fate specification. Later on, it was reported to affect the size of the primary lymph sacs and the patterning and the maintenance of the lymphatic vasculature, whereas in mature lymphatic endothelial cells NFATc1 was also reported to induce the expression of certain lymphatic endothelial genes (Kulkarni et al., 2009).

On the other hand, the lack of regulation by BMP9 of the expression of the transcription factors *Coup-tfII*, *Sox18*, and *Prox-1*, known to be crucial in the first steps of lymphatic development, indicates that BMP9 probably regulates a population of lymphatic progenitors and/or more distal checkpoints in the commitment of the lymphatic specification. These results are in accordance with the BMP9-induced proliferative effect on an early specified LYVE-1-positive cell population.

Expression analysis during early mouse embryo development demonstrated that BMP9 is detected from E10 (Chen et al., 2013). This timing of expression is compatible with a potential role during lymphatic specification and development that starts at E9.5 for veins or from E12.5 to E13.5 for other embryonic non-venous origins (for review, see Kazenwadel and Harvey, 2016). Nonetheless, further experiments remain to be done to fully establish that BMP9 constitutes a key regulator of the initial steps of mouse lymphatic development *in vivo*.

During ESC-derived vascular precursor differentiation, high BMP9 concentrations were observed to increase CD31$^+$ LYVE-1$^-$ endothelial cell formation. Our data are consistent with an indirect effect relayed by OP9 stromal cells via ALK2, which respond to high BMP9

concentrations by expressing and secreting VEGF-A. Our results provide further evidence, as described in rat mesenchymal stem cells (Ai et al., 2015), that *Vegf-A* constitutes a BMP9 target gene.

This study combined with our previous data (Levet et al., 2013) reveals that BMP9 may act at several different steps of mouse lymphatic endothelial development: first, being pro-lymph-vasculogenic during the initiation process, and later on regulating the lymphatic vessel maturation and valve formation processes. It should be noted that during the first steps of lymphatic development, the BMP9 signal intensity appears of great importance in defining the endothelial cell fate of the vascular precursor cells. A potential BMP9 involvement in the regulation of endothelial cell plasticity in adult stages has also been recently discussed (Derynck and Akhurst, 2013; Yoshimatsu et al., 2013). This adds another level of regulation for BMP9, whose effects appear variable and dependent on the lymphatic maturation stage.

It is currently accepted that BMPs bind to a tetrameric receptor complex composed of two type I and two type II receptors (for review, see Morrell et al., 2016). Previous reports have established that BMP9 activates both ALK1 and ALK2 (for review, see Goumans et al., 2018). The BMP9 vascular endothelial effects have been in large part linked with the activation of ALK1, whereas its potent osteogenic effect appears mainly mediated by the activation of ALK2 (Garcia de Vinuesa et al., 2016; Lamplot et al., 2013). The endothelial differentiation of adipocyte-derived multipotent cells treated by 10 ng/mL BMP9 was also described to involve ALK2 (Jumabay et al., 2012). In this study, we provide evidence that the differential BMP9 effects observed, according to dosage, are the consequence of the mobilization of specific type I receptors. Indeed, the RNA-silencing experiment results are consistent with the involvement of the ALK1 high-affinity BMP9 receptor in the response to low BMP9 doses and of the further mobilization of ALK2 for the high BMP9 concentrations. Interestingly, some recent studies reported that BMP signaling by ALK3 is essential for the zebrafish lymphatic development (Kim and Kim, 2014), and that 10 ng/mL BMP9 activates SMAD1/5 phosphorylation via ALK3 in PA1 breast cancer cells (Varadaraj et al., 2015). Further work then appears necessary to characterize whether ALK3 may also be involved in the endothelial lymphatic effects of BMP9.

The fact that BMP9 constitutes an early driver for the lymphatic lineage expansion during mouse ESC *in vitro* differentiation appears of great interest to further establish *in vitro* protocols aimed at amplifying lymphatic derivatives from stem cells for cell-replacement strategies. However, these data need to be confirmed in human stem cells. Indeed, despite similar responses, such as the negative BMP2 effect on lymphatic differentiation, some differences in BMP signaling between mouse and human ESCs could exist, as described during ESC self-renewal (for review, see Li and Chen, 2013). Some differences in the timing of the events and in the lymphatic fate specification regulating pathways may also exist, as described between mouse and zebrafish (Koltowska et al., 2015; van Impel et al., 2014).

The generation of lymphatic endothelial cells has already been reported from human ESCs or induced pluripotent stem cells during co-culture experiments with the OP9 murine stromal cell line (Lee et al., 2015). In the light of all our results, the combination of TGFβ and VEGF-A inhibition along with BMP9 stimulation may potentially be particularly useful for expansion of the lymphatic endothelial cell population. This combination may improve lymphatic differentiation from human stem cells, such as adipose-derived stem cells. Future investigations should be performed in this way since the identification of the basic fundamental mechanisms involved in human lymph-vasculogenesis may be of further interest in elaborating novel perspectives of cell therapies for the treatment of lymphedema.

## EXPERIMENTAL PROCEDURES

### Cell Culture and ESC Differentiation

OP9 stromal cells were obtained from the American Type Culture Collection (Manassas, VA). They were cultured in α-modified Eagle's medium (αMEM) supplemented with 20% fetal calf serum and 1% non-essential amino acids, according to the recommendations of the manufacturer.

Murine CJ7 ESCs (Swiatek and Gridley, 1993) (a gift from Dr. T. Gridley, The Jackson Laboratory, Bar Harbor, ME) were used. They were cultured and differentiated into embryoid bodies as previously described (Prandini et al., 2007; Vittet et al., 2012). Embryoid bodies were harvested after 5 days of differentiation and were dissociated in non-enzymatic cell dissociation buffer (Life Technologies). After staining with a phycoerythrin (PE)-conjugated rat monoclonal antibody against mouse FLK-1 (BD Pharmingen), FLK-1-positive cells were sorted using either a MoFlo FACS cell sorter (DAKO Cytomation, Glostrup, Denmark) or a BD FACS Melody cell sorter (BD Biosciences), and subcultured on an OP9 cell stromal feeder layer as previously described (Vittet et al., 2012). When tested, BMPs and other agents were added at day 6 in serum-free X-vivo15 medium (Lonza Biosciences, Basel, Switzerland). Early lymphatic specification was quantified at day 10 by fluorescence-activated cell sorting (FACS) analysis of LYVE-1-positive cell formation.

Human recombinant BMPs, normal goat immunoglobulin G (AB-108-C), and neutralizing goat anti-mouse VEGF-$A_{164}$ antibody (AF-493-NA) were purchased from BioTechne. Recombinant human VEGF-$A_{165}$ and human fibroblast growth factor 2 were from PromoCell (Heidelberg, Germany). All other standard culture reagents were from Life Technologies.

## Immunofluorescent Stainings

Indirect immunofluorescence experiments on cells cultured in chamber culture slides were performed as previously described (Vittet et al., 2012). The images were acquired using either a Zeiss Axio-Observer Z1 inverted fluorescence microscope and Axiovision 4.8 software, or a Zeiss Axio-Imager 2 fluorescence microscope equipped with an apotome and ZEN software. All images were processed with Adobe Photoshop CS5 software.

## FACS

For FACS analysis of endothelial differentiation, cells were detached from the plates using non-enzymatic cell dissociation buffer, as described by Vittet et al. (2012). After two washes with PBS, they were first incubated with LYVE-1 antibody (BioTechne, AF2125) followed by a mixture of PE-conjugated rat anti-mouse CD31 (BD Pharmingen) and Alexa 488-conjugated donkey anti-goat antibodies (Jackson ImmunoResearch Laboratories, West Grove, PA). Cells were then analyzed on a FacsCalibur flow cytometer (BD Biosciences) using CellQuest software (BD Biosciences). For $CD31^+$ $LYVE\text{-}1^+$, $CD31^+$ $LYVE\text{-}1^-$, and $CD31^-$ $LYVE\text{-}1^-$ cell population sorting, detached cells from the co-cultures were incubated with a mixture of PE-conjugated rat anti-mouse CD31 and APC-conjugated rat anti-mouse LYVE-1 (BioTechne, FAB2125A).

For the analysis of the proliferative status of cells, co-cultures were pulse labeled with 10 μM BrdU for 1 hr. After cell recovery as described above and first labeling of cell surface LYVE-1 antigens, the immunofluorescent staining of incorporated BrdU was achieved using the APC BrdU Flow kit (BD Pharmingen) according to the manufacturer's recommended protocol.

## Real-Time qPCR

In co-culture experiments, confluent layers of OP9 cells were first stained with the long-term fluorescent CellTracker Green CMFDA (5-chloromethylfluorescein diacetate) (Molecular Probes, Eugene, OR) before plating $FLK\text{-}1^+$ vascular precursors. After 24-hr treatment with 0.3 ng/mL BMP9 in serum-free medium, the CMFDA-negative fraction was sorted for gene expression analysis.

For gene expression studies, total RNA was extracted from cells using a Nucleospin RNA XS kit (Macherey-Nagel, Düren, Germany) and first-strand cDNA was synthesized from 1 μg of total RNA by reverse transcription using the iScript System (Bio-Rad Laboratories, Hercules, CA) according to the manufacturer's instructions. Real-time qPCR was performed using a C1000 thermal cycler with a CFX96 real-time PCR detection system (Bio-Rad) and the ready-to-use GoTaq QPCR Master Mix (Promega) according to the manufacturer's instructions. Values obtained for each gene were normalized to hypoxanthine phosphoribosyltransferase (*Hprt*) mRNA expression level for relative quantification. The primer sequences used are listed in Table S1.

## Protein Extraction and Western Blot Analysis

Sorted $FLK\text{-}1^+$ vascular precursors or OP9 stromal cells were stimulated in suspension in PBS buffer for 1 hr with the different BMP9 concentrations. They were then lysed in RIPA buffer (pH 7.4) (50 mM Tris-HCl, 150 mM NaCl, 0.5% deoxycholate, 0.1% SDS, 1% NP40). Proteins were separated on SDS-PAGE 4%–20% gels (Bio-Rad, Mini Protean TGX Stain Free) and immunoblots were performed with rabbit anti-phospho-SMAD1/5 (Cell Signaling Technologies, 41D10) or mouse anti-NFATc1 (BD Biosciences, clone 7A6) and β-actin (Sigma, AC-15), or GAPDH (Applied Biosystems, Ambion #AM4300) primary antibodies for the control of protein loading.

## VEGF-A ELISA

The VEGF-A levels in the culture medium were measured using a mouse $VEGF\text{-}A_{164}$ ELISA kit (BioTechne; Mouse VEGF Quantikine ELISA Kit, MMV00) according to the manufacturer's instructions.

## RNA-Silencing Experiments

$FLK\text{-}1^+$ vascular precursors in co-culture on OP9 cell layer since 24 hr and adherent OP9 cells were transfected with 10 nM siRNA using Lipofectamine RNAiMAX transfection reagent (Life Technologies) according to the manufacturer's instructions. Stimulation with BMP9 was performed 24 hr after transfection in serum-free medium. In some experiments, $FLK\text{-}1^+$ vascular precursors were transfected in cell suspension by improved electroporation using the Nucleofector technology with the Amaxa device and the optimized protocol developed for stem cells (Lonza). Transfected cells were then plated in co-culture on OP9 stromal cells for 24 hr before stimulation with or without BMP9 for further differentiation study analysis.

siRNAs were purchased from Ambion (*Alk1*, #s986, *Alk2*, #s61924, and siRNA Scramble [*Scr*], AM4613).

## Statistics

Values are presented as mean ± SEM. The results were analyzed by unpaired Student's t test.

## SUPPLEMENTAL INFORMATION

Supplemental Information includes four figures and one table and can be found with this article online at https://doi.org/10.1016/j.stemcr.2018.11.024.

## AUTHOR CONTRIBUTIONS

M.S., G.M., and D.V. designed and performed research; D.C. took part in the performing of qRT-PCR experiments; V.C-F. performed cell-sorting experiments; M.S., J.-J.F., S.B., and D.V. discussed the results; D.V. wrote the manuscript with the help of M.S.

## ACKNOWLEDGMENTS

The authors thank Mr. Stephane Hasse for his participation in the PCR experiments. This research work was supported by Inserm (U1036), CEA (BIG/BCI), UGA, AMRO-HHT France, and the Fondation ARC (grant no. PJA 20131200252).

Received: July 4, 2016
Revised: November 30, 2018
Accepted: November 30, 2018
Published: December 27, 2018

## REFERENCES


Ai, W.J., Li, J., Lin, S.M., Li, W., Liu, C.Z., and Lv, W.M. (2015). R-smad signaling-mediated VEGF expression coordinately regulates endothelial cell differentiation of rat mesenchymal stem cells. Stem Cells Dev. *24*, 1320–1331.

Aspelund, A., Robciuc, M.R., Karaman, S., Makinen, T., and Alitalo, K. (2016). Lymphatic system in cardiovascular medicine. Circ. Res. *118*, 515–530.

Chen, H., Brady Ridgway, J., Sai, T., Lai, J., Warming, S., Roose-Girma, M., Zhang, G., Shou, W., and Yan, M. (2013). Context-dependent signaling defines roles of BMP9 and BMP10 in embryonic and postnatal development. Proc. Natl. Acad. Sci. U S A *110*, 11887–11892.

Cunha, S.I., Magnusson, P.U., Dejana, E., and Lampugnani, M.G. (2017). Deregulated TGF-beta/BMP signaling in vascular malformations. Circ. Res. *121*, 981–999.

David, L., Mallet, C., Mazerbourg, S., Feige, J.J., and Bailly, S. (2007). Identification of BMP9 and BMP10 as functional activators of the orphan activin receptor-like kinase 1 (ALK1) in endothelial cells. Blood *109*, 1953–1961.

Derynck, R., and Akhurst, R.J. (2013). BMP-9 balances endothelial cell fate. Proc. Natl. Acad. Sci. U S A *110*, 18746–18747.

Dunworth, W.P., Cardona-Costa, J., Bozkulak, E.C., Kim, J.D., Meadows, S., Fischer, J.C., Wang, Y., Cleaver, O., Qyang, Y., Ober, E.A., et al. (2014). Bone morphogenetic protein 2 signaling negatively modulates lymphatic development in vertebrate embryos. Circ. Res. *114*, 56–66.

Garcia de Vinuesa, A., Abdelilah-Seyfried, S., Knaus, P., Zwijsen, A., and Bailly, S. (2016). BMP signaling in vascular biology and dysfunction. Cytokine Growth Factor Rev. *27*, 65–79.

Goumans, M.J., Zwijsen, A., Ten Dijke, P., and Bailly, S. (2018). Bone morphogenetic proteins in vascular homeostasis and disease. Cold Spring Harb. Perspect. Biol. *10*, a022210.

Horsley, V., and Pavlath, G.K. (2002). NFAT: ubiquitous regulator of cell differentiation and adaptation. J. Cell Biol. *156*, 771–774.

Jakobsson, L., Kreuger, J., and Claesson-Welsh, L. (2007). Building blood vessels—stem cell models in vascular biology. J. Cell Biol. *177*, 751–755.

Jiang, X., Nicolls, M.R., Tian, W., and Rockson, S.G. (2018). Lymphatic dysfunction, leukotrienes, and lymphedema. Annu. Rev. Physiol. *80*, 49–70.

Jumabay, M., Abdmaulen, R., Urs, S., Heydarkhan-Hagvall, S., Chazenbalk, G.D., Jordan, M.C., Roos, K.P., Yao, Y., and Bostrom, K.I. (2012). Endothelial differentiation in multipotent cells derived from mouse and human white mature adipocytes. J. Mol. Cell. Cardiol. *53*, 790–800.

Kazenwadel, J., and Harvey, N.L. (2016). Morphogenesis of the lymphatic vasculature: a focus on new progenitors and cellular mechanisms important for constructing lymphatic vessels. Dev. Dyn. *245*, 209–219.

Kim, J.D., and Kim, J. (2014). Alk3/Alk3b and Smad5 mediate BMP signaling during lymphatic development in zebrafish. Mol. Cell *37*, 270–274.

Koltowska, K., Lagendijk, A.K., Pichol-Thievend, C., Fischer, J.C., Francois, M., Ober, E.A., Yap, A.S., and Hogan, B.M. (2015). Vegfc regulates bipotential precursor division and prox1 expression to promote lymphatic identity in zebrafish. Cell Rep. *13*, 1828–1841.

Kono, T., Kubo, H., Shimazu, C., Ueda, Y., Takahashi, M., Yanagi, K., Fujita, N., Tsuruo, T., Wada, H., and Yamashita, J.K. (2006). Differentiation of lymphatic endothelial cells from embryonic stem cells on OP9 stromal cells. Arterioscler. Thromb. Vasc. Biol. *26*, 2070–2076.

Kreuger, J., Nilsson, I., Kerjaschki, D., Petrova, T., Alitalo, K., and Claesson-Welsh, L. (2006). Early lymph vessel development from embryonic stem cells. Arterioscler. Thromb. Vasc. Biol. *26*, 1073–1078.

Kulkarni, R.M., Greenberg, J.M., and Akeson, A.L. (2009). NFATc1 regulates lymphatic endothelial development. Mech. Dev. *126*, 350–365.

Lamplot, J.D., Qin, J., Nan, G., Wang, J., Liu, X., Yin, L., Tomal, J., Li, R., Shui, W., Zhang, H., et al. (2013). BMP9 signaling in stem cell differentiation and osteogenesis. Am. J. Stem Cells *2*, 1–21.

Lee, S.J., Park, C., Lee, J.Y., Kim, S., Kwon, P.J., Kim, W., Jeon, Y.H., Lee, E., and Yoon, Y.S. (2015). Generation of pure lymphatic endothelial cells from human pluripotent stem cells and their therapeutic effects on wound repair. Sci. Rep. *5*, 11019.

Levet, S., Ciais, D., Merdzhanova, G., Mallet, C., Zimmers, T.A., Lee, S.J., Navarro, F.P., Texier, I., Feige, J.J., Bailly, S., et al. (2013). Bone morphogenetic protein 9 (BMP9) controls lymphatic vessel maturation and valve formation. Blood *122*, 598–607.

Li, Z., and Chen, Y.-G. (2013). Functions of BMP signaling in embryonic stem cell fate determination. Exp. Cell Res. *319*, 113–119.

Liersch, R., Nay, F., Lu, L., and Detmar, M. (2006). Induction of lymphatic endothelial cell differentiation in embryoid bodies. Blood *107*, 1214–1216.

Ma, W., and Oliver, G. (2017). Lymphatic endothelial cell plasticity in development and disease. Physiology *32*, 444–452.

Matsumura, K., Hirashima, M., Ogawa, M., Kubo, H., Hisatsune, H., Kondo, N., Nishikawa, S., and Chiba, T. (2003). Modulation of VEGFR-2-mediated endothelial-cell activity by VEGF-C/VEGFR-3. Blood *101*, 1367–1374.

Morrell, N.W., Bloch, D.B., ten Dijke, P., Goumans, M.J., Hata, A., Smith, J., Yu, P.B., and Bloch, K.D. (2016). Targeting BMP signalling in cardiovascular disease and anaemia. Nat. Rev. Cardiol. *13*, 106–120.

Murtomaki, A., Uh, M.K., Choi, Y.K., Kitajewski, C., Borisenko, V., Kitajewski, J., and Shawber, C.J. (2013). Notch1 functions as a negative regulator of lymphatic endothelial cell differentiation in the venous endothelium. Development *140*, 2365–2376.

Niessen, K., Zhang, G., Ridgway, J.B., Chen, H., and Yan, M. (2010). ALK1 signaling regulates early postnatal lymphatic vessel development. Blood *115*, 1654–1661.

Norrmen, C., Ivanov, K.I., Cheng, J., Zangger, N., Delorenzi, M., Jaquet, M., Miura, N., Puolakkainen, P., Horsley, V., Hu, J., et al. (2009). FOXC2 controls formation and maturation of lymphatic collecting vessels through cooperation with NFATc1. J. Cell Biol. *185*, 439–457.

Prandini, M.H., Desroches-Castan, A., Feraud, O., and Vittet, D. (2007). No evidence for vasculogenesis regulation by angiostatin during mouse embryonic stem cell differentiation. J. Cell. Physiol. *213*, 27–35.

Qi, S., and Pan, J. (2015). Cell-based therapy for therapeutic lymphangiogenesis. Stem Cells Dev. *24*, 271–283.

Rostama, B., Turner, J.E., Seavey, G.T., Norton, C.R., Gridley, T., Vary, C.P., and Liaw, L. (2015). DLL4/Notch1 and BMP9 interdependent signaling induces human endothelial cell quiescence via P27KIP1 and thrombospondin-1. Arterioscler. Thromb. Vasc. Biol. *35*, 2626–2637.

Scharpfenecker, M., van Dinther, M., Liu, Z., van Bezooijen, R.L., Zhao, Q., Pukac, L., Lowik, C.W., and ten Dijke, P. (2007). BMP-9 signals via ALK1 and inhibits bFGF-induced endothelial cell proliferation and VEGF-stimulated angiogenesis. J. Cell Sci. *120*, 964–972.

Semo, J., Nicenboim, J., and Yaniv, K. (2016). Development of the lymphatic system: new questions and paradigms. Development *143*, 924–935.

Shaitelman, S.F., Cromwell, K.D., Rasmussen, J.C., Stout, N.L., Armer, J.M., Lasinski, B.B., and Cormier, J.N. (2015). Recent progress in the treatment and prevention of cancer-related lymphedema. CA Cancer J. Clin. *65*, 55–81.

Sieber, C., Kopf, J., Hiepen, C., and Knaus, P. (2009). Recent advances in BMP receptor signaling. Cytokine Growth Factor Rev. *20*, 343–355.

Suzuki, Y., Ohga, N., Morishita, Y., Hida, K., Miyazono, K., and Watabe, T. (2010). BMP-9 induces proliferation of multiple types of endothelial cells in vitro and in vivo. J. Cell Sci. *123*, 1684–1692.

Swiatek, P.J., and Gridley, T. (1993). Perinatal lethality and defects in hindbrain development in mice homozygous for a targeted mutation of the zinc finger gene Krox20. Genes Dev. *7*, 2071–2084.

Toyserkani, N.M., Christensen, M.L., Sheikh, S.P., and Sorensen, J.A. (2015). Stem cells show promising results for lymphoedema treatment–a literature review. J. Plast. Surg. Hand Surg. *49*, 65–71.

van Impel, A., Zhao, Z., Hermkens, D.M., Roukens, M.G., Fischer, J.C., Peterson-Maduro, J., Duckers, H., Ober, E.A., Ingham, P.W., and Schulte-Merker, S. (2014). Divergence of zebrafish and mouse lymphatic cell fate specification pathways. Development *141*, 1228–1238.

Varadaraj, A., Patel, P., Serrao, A., Bandyopadhay, T., Lee, N.Y., Jazaeri, A.A., Huang, Z., Murphy, S.K., and Mythreye, K. (2015). Epigenetic regulation of GDF2 suppresses anoikis in ovarian and breast epithelia. Neoplasia *17*, 826–838.

Vittet, D., Merdzhanova, G., Prandini, M.H., Feige, J.J., and Bailly, S. (2012). TGFbeta1 inhibits lymphatic endothelial cell differentiation from mouse embryonic stem cells. J. Cell. Physiol. *227*, 3593–3602.

Yoshimatsu, Y., Lee, Y.G., Akatsu, Y., Taguchi, L., Suzuki, H.I., Cunha, S.I., Maruyama, K., Suzuki, Y., Yamazaki, T., Katsura, A., et al. (2013). Bone morphogenetic protein-9 inhibits lymphatic vessel formation via activin receptor-like kinase 1 during development and cancer progression. Proc. Natl. Acad. Sci. U S A *110*, 18940–18945.